Manuscript prepared for Earth Syst. Sci. Data
with version 2015/09/17 7.94 Copernicus papers of the LaTeX class copernicus.cls.
Date: 6 August 2017

Using CALIOP to estimate the base height of optically thick clouds

Johannes Mülmenstädt[1], Odran Sourdeval[1], Tristan L'Ecuyer[2], Christoph Böhm[3], and Johannes Quaas[1]

[1]Institute of Meteorology, Universität Leipzig, Leipzig, Germany
[2]University of Wisconsin, Madison, USA
[3]Institute of Meteorology, Universität Köln, Köln, Germany

Correspondence to: Johannes Mülmenstädt (johannes.muelmenstaedt@uni-leipzig.de)

Abstract. A measurement technique is presented that uses CALIOP lidar profiles to estimate cloud base heights. The technique provides cloud base heights even when clouds are thick enough to attenuate the lidar beam (optical thickness $\tau \gtrsim 5$) by treating the cloud base height of nearby thinner clouds as representative of the entire cloud field. Using ground-based ceilometer data, uncertainty estimates are derived as a function of various properties of the CALIOP lidar profiles. Evaluation of the predicted cloud base heights and their predicted uncertainty using a second, statistically independent, ceilometer data set shows that cloud base heights and uncertainties are biased by less than 10%. Geographic distributions of cloud base height and its uncertainty are presented. {j_μ: Regionally, the uncertainty is found to be substantially smaller than the 480 m uncertainty assumed in the A-Train downwelling longwave estimate, potentially permitting the most uncertain of the radiative fluxes in the climate system to be much better constrained.}

1 Introduction

Cloud base height (CBH) is an important geometric parameter of a cloud. It controls how much downwelling longwave radiation the cloud emits. Aerosol concentration and updraft speed at that level control the microphysics of the cloud. It is one of the parameters that is required in the calculation of the subadiabaticity of the cloud. However, due to the viewing geometry, it is also one of the most difficult parameters to retrieve from satellite.

Multiple methods have been proposed for satellite determination of the cloud base height. VIIRS cloud-base temperature method: zhu. Results of evaluating CBH inferred from oxygen absorption bands and from MISR stereoscopic images will be reported in separate manuscripts. For analyses wishing to combine cloud base information with other cloud properties retrieved by A-Train satellites, these methods share the disadvantage that the required instruments are not part of the A-Train. Methods that are applicable to A-Train satellites are based on MODIS cloud properties retrieved near cloud top and integrated along moist adiabats to determine the cloud thickness (mee) or on active

remote sensing by CloudSat (mar, 2B-GEOPROF) or a combination of CloudSat and CALIOP (mac, 2B-GEOPROF-LIDAR). The MODIS-derived cloud thickness assumes adiabatic cloud profiles and therefore cannot be used to constrain subadiabaticity. CloudSat misses the small droplets at the base of nonprecipitating clouds, and retrievals are further degraded in the ground clutter region. CALIOP detects the bases of only the thinnest clouds (mac, $\tau < 5$); frequently, it is desirable to know the base height of thick clouds as well.

In this paper, we revisit the CALIOP cloud base determination. Because the lifting condensation level is approximately homogeneous within an airmass, the cloud bases retrieved by CALIOP for thin clouds may be a good proxy for the cloud base heights of an entire cloud field, including the optically thicker clouds within the filed. We have designed an algorithm that extrapolates the CALIOP cloud-base measurements into locations where CALIOP attenuates before reaching cloud base. This algorithm is called CBASE (Cloud Base Altitude Spatial Extrapolator). In this paper we evaluate its performance by comparing CBASE CBH against CBH observed by ground-based ceilometers.

Section 2 describes the data sources used in determining and evaluating CBH. In Section 3 we describe the algorithm and evaluate its performance, including error statistics. The publicly available processed CBASE output is described in Section 4. We conclude in Section 5 with an outlook on the longstanding questions that the CBASE data set can address.

2 Data

Two classes of data are used in this work. The first class is satellite data, which we use with the intent of deriving a global CBH data set. The second class is ground-based observations of "true" CBH used to train and evaluate the algorithm by which CBH is determined from the satellite data.

2.1 CALIOP VFM

The input satellite data to our analysis is the CALIOP vertical feature mask (VFM). For each CALIOP lidar backscatter profile, the VFM identifies features such as clear air, cloud, aerosol, or planetary surface; this is termed the "feature type". In addition to the feature type, the VFM records the degree of confidence in the identification ("none" to "high", termed the "feature type QA flag"); the thermodynamic phase of a layer identified as cloud as well as the degree of confidence therein (termed "ice water phase" and "ice water phase QA flag"); the horizontal distance over which the algorithm had to average to identify a feature above noise and molecular atmospheric scattering ("horizontal averaging distance").

In the present analysis, we use VFM version 4.10 (CALIPSO Science Team, 2016), the current "standard" release. The VFM files are obtained from ICARE (**?**).

2.2 Airport ceilometers

For optimizing several parameters of the algorithm, for determining the expected cloud base uncertainty, and for evaluation of the trained algorithm, the "true" CBH needs to be known. The source of the "true" CBH in this work is ground-based cloud observations in aviation routine and special weather reports (World Meteorological Organization, 2013, METARs and SPECIs, collectively referred to as METARs henceforth). METAR data is used, among other purposes, for assimilation in NWP (HRR; IFS, e.g.,). In many locations, CBH reported in METARs are measured by ceilometer over a period of time (tens of minutes) and then objectively grouped into cloud layers and their respective fractional coverages, using the temporal variation at a fixed point under an advected cloud field as a proxy for spatial variability of the cloud field. METAR data is distributed globally by the WMO and widely archived. The data for the present analysis was downloaded from the Weather Underground archive (**?**).

To ensure that the ceilometer CBH are of high and spatially uniform quality, we restrict ourselves to METARs from the contiguous continental United States, where the CBH is mostly derived automatically by laser ceilometers that form part of Automated Surface Observing Stations (National Oceanic and Atmospheric Administration, Department of Defense, Federal Aviation Administration, and United States Navy, 1998, ASOS) system. In other parts of the world, the cloud bases may be estimated by human observers or may be omitted under certain conditions when the lowest cloud base is higher than 5000 feet.

3 CBASE Algorithm and evaluation

The CBASE algorithm and evaluation proceed in four steps:

1. We determine the CBH from all CALIOP profiles where the surface generates a return, indicating that the lidar is not completely attenuated by cloud. We refer to this as the *local CBH* in the sense that it is local to the CALIOP profile.

2. Using ground-based ceilometer data, we determine quality of cloud base height depending on a number of properties of the CALIOP profile; assuming those properties suffice to determine the quality of the CBH determination, we can then predict the uncertainty of a cloud base as a function of those factors. In the language of machine learning, we refer to this step as *training* the algorithm on the ceilometer data.

3. Based on the predicted quality of each local cloud base, we either reject the local cloud base or combine it with other local cloud bases within a distance $D_{\max}$ of the point of interest (POI) to arrive at an estimate of the CBH and its uncertainty at the POI.

4. Using a statistically independent validation dataset, we verify that the predicted CBH and its uncertainty are correct.

At several points in the algorithm development, it is necessary to know the true (ceilometer-observerd) CBH. We use ceilometer observations from the year 2008 at those points. A statistically independent data set is required for an unbiased evaluation of the algorithm performance; we use the year 2007 for evaluation.

This section is divided into four subsections, one for each algorithm step enumerated above.

3.1 Determination of local CBH

Local CBH is determined from the CALIOP VFM for each profile with a surface return. Figure 1 illustrates the method.

3.2 Determination of local cloud base quality

We assess the quality of the CALIOP CBH z from the ceilometer-observed CBH $\hat{z}$ using root mean square error (RMSE), defined as

$$E = \sqrt{\frac{1}{N}\sum_{i=1}^{N}(z_i - \hat{z})^2}. \tag{1}$$

The sum runs over all CALIOP profiles containing a cloud layer and a surface return that are within 100 km horizontal distance of the ceilometer, occurred within 3600 s of a ceilometer observation, and have their lowest CALIOP cloud feature within 3 km of the surface. Ceilometer observations are only used if the observation closest in time to the Calipso overpass contains a cloud within 3 km of the surface. A height limit is imposed because a subset of the ceilometers has a range limit of 12500 feet, and all ceilometers report ceilings above 10000 feet with reduced granularity (500 feet); the 3 km threshold avoids those ceilometer limitations and mimics the ISCCP definition of low cloud ($p > 690$ hPa).

The following metrics, which are useful for a qualitative assessment of the quality of the satellite cloud base, are also calculated, but play no quantitative role in the algorithm:

Correlation coefficient between the CALIOP cloud base and ground-based observation of the cloud base. We use the Pearson correlation coefficient. Ideally the correlation coefficient would be unity.

Linear regression slope and intercept (ideally 1 and 0, respectively).

Retrieval bias, defined as

$$\text{bias} = \frac{1}{N}\sum_{i=1}^{N}(z_i - \hat{z}), \tag{2}$$

(ideally 0)

Efficiency, i.e., probability that a retrieval is available at the desired location (ideally 1).

CALIOP's ability to detect cloud base depends on the properties of the cloud. Therefore, we expect that the CBH quality will vary between different cloud profiles. Measuring the quality as a function of various properties of the CALIOP column may allow us to predict the quality of other columns with the same combination of properties. The properties that are easily accessible in a single column and have the greatest effect on quality are:

- horizontal distance D from the ceilometer,
- number of column cloud bases within horizontal distance $D_{\max}$,
- CALIOP VFM feature quality assurance flag,
- geometric thickness of the lowest cloud layer,
- CALIOP thermodynamic phase determination of lowest cloud,
- feature type, if any, detected between the lowest cloud and the surface,
- and horizontal averaging distance required for CALIOP cloud feature detection.

For illustrative purposes, Figure 2 shows the joint distribution of CALIOP and ceilometer CBH faceted by the CALIOP VFM feature quality assurance flag.

Based on determining the retrieval quality one variable at a time, the following classes of CALIOP profiles are discarded:

- CALIOP VFM quality assurance worse than "high" ,
- "invalid" or "no signal" layers between the surface and the lowest cloud layer (indicating that although the surface may generate a detectable return, the lidar is sufficiently attenuated that the cloud base, which scatters less strongly than the surface, is unreliable),
- minimum CALIOP cloud detection horizontal averaging distance within the lowest cloud layer greater than 1 km,
- or phase of the lowest layer determined to be other than liquid by the CALIOP VFM algorithm (the reason for this is that not enough such columns exist to determine the RMSE reliably in each of the categories defined below).

The remaining variables are discretized roughly into quintiles with the following boundaries:

- horizontal distance D from the ceilometer, with boundaries 0, 40, 60, 75, 88, and 100 km (distance greater than 100 km is discarded),
- number of CALIOP columns n with a cloud layer and a surface return within 100 km horizontal distance from the ceilometer, with boundaries at 0, 175, 250, 325, 400 (multiplicities greater than 400 are accepted),

– geometric thickness Δz of the lowest cloud layer, with boundaries at 0, 0.25, 0.45, 0.625, and 1 km (thickness greater than 1 km is accepted).

We can now consider the joint distribution of CALIOP and ceilometer cloud bases for each combination of the above variables. (Base heights above ground are used to remove an intrinsic correlation due to terrain.) Because of the viewing geometry, high CALIOP cloud bases tend to be overestimates where a higher layer obscures a lower layer. {j_μ: Isn't the actual reason a combination of regression dilution at the extremes of the distribution and phase space truncation at a physical boundary for low cloud bases?} It is desirable to correct for this bias. The options are no correction, a linear correction (which partially corrects for the high bias of high CALIOP base heights but introduces a counterbias at low CALIOP base heights), and a nonlinear correction that does not suffer from the counterbias at low CALIOP base heights. Our choice for nonlinear correction is a support vector machine. The final choice of correction is based on the performance of the three options on the training sample after combination has been performed according to the next step of the algorithm (Section 3.3).

Following bias correction, the sample RMSE is calculated for each combination of D, n, and Δz. The sample RMSE is taken as an estimate of the statistical uncertainty $\sigma(D, n, \Delta z)$ on the CALIOP CBH.

3.3 Combination of local cloud bases

CALIOP CBH only exists sporadically {j_μ: (on average x% of columns)}, when CALIOP happens to hit a sufficiently thin cloud. To infer the CBH z at a point of interest (POI) that does not necessarily coincide with the location of a thin-cloud CALIOP profile, we proceed as follows. We first select all local CALIOP CBH measurements within a horizontal distance $D_{\max} = 100$ km of the POI that satisfy the additional quality cuts described in Section 3.2.

For each remaining local CBH z_i, we determine the predicted uncertainty σ_i based on the categories established in the previous section. We determine a combined CBH

$$z = \frac{\sum_i^n w_i z_i}{\sum_i^n w_i} \tag{3}$$

with weights

$$w_i = \frac{1}{\sigma_i^2} \tag{4}$$

(optimal weights for uncorrelated least-squares). In practice, the individual measurements of cloud base are highly correlated with fairly similar σ_i. The cloud base estimate by Eq. (3) with weights given by Eq. (4) remains unbiased even in the presence of correlations. However, for the combined cloud base uncertainty, the uncorrelated weights would yield a biased estimate in the presence of

correlations. The expression

$$\sigma^2 = \frac{1}{n}\sum_{i}^{n}\sigma_i^2 \tag{5}$$

yields acceptable results, as would be expected for highly correlated and fairly similar σ_i. {j_μ: This i could be confused with the i in the previous section; rethink notation.}

One choice remains to be made, namely which of the bias correction methods described in Section 3.2 to apply to the local cloud base heights before combination. Combining the uncorrected local base heights result in a high bias (Figure S1), as would be expected from the high bias on the constituent local CBH. The linear correction, which reduces the high bias for high CBH but introduces a counterbias for low cloud base heights, leads to a low bias in the combined base height (Figure S2), again as would be expected. Among the correction methods investigated, the SVM-based correction results in the behavior closest to the 1-to-1 line (Figure S3). Based on this performance, we use the SVM-corrected local base heights as input to combination step of the CBASE algorithm.

3.4 Evaluation of CBH and CBH errors

Having trained the algorithm on data from the year 2008, we evaluate it using a statistically independent data set from the year 2007. In the evaluation data set, the "true" (i.e., ceilometer-measured) CBH $\hat{z}$ is known in addition to the estimated CBH z and the estimated CBH uncertainty σ, determined according to the procedure described in the previous section. Figure 3 shows the joint distribution of CBASE and ceilometer-observed CBH. (The difference between this figure and Figure S3 is that the underlying data is the validation, rather than the training, data set.)

For satellite-derived measurements of the CBH z that are unbiased with respect to the ceilometer-observed CBH $\hat{z}$ and have correctly estimated uncertainties σ, the pdf of the quantity $(z-\hat{z})/\sigma$ has zero mean and unit standard deviation. In our evaluation data set, we find a mean of 0.04 and a standard deviation of 1.06, shown in Figure 4; this corresponds to a CBH bias of 4% and uncertainty bias of 6%, both relative to the predicted uncertainty. Thus, we find that both the cloud base estimate and the uncertainty estimate are unbiased at the better than 10% level.

As a further test of the reliability of the expected uncertainty, we divide the validation data set into deciles of the expected uncertainty. Table 2 shows that the actual RMSE within each decile is within 10% of the expected uncertainty and that linear regressions within each decile are close to the one-to-one line.

It is possible that CBH estimates outside North America could have greater biases or that greater uncertainty than this evaluation leads us to believe. This would be the case if continental clouds over North America are not representative of clouds elsewhere in a way that is not accounted for by the cloud properties taken into account by the uncertainty estimate. Since the validation sample spans an entire year on a continental scale, we expect that most cloud morphologies are included. However, certain cloud types exist that occur predominantly over ocean and present a particular challenge

to the method, namely marine stratocumulus with horizontally extensive but vertically thin liquid-phase anvils. Due to the typical CBH uncertainty of several hundred m, the method is unlikely to be applied to stratocumulus cloud; nevertheless, a marine-cloud validation data set would be desirable. For the present work, no suitable marine-cloud evaluation data set was available; ship-based CBH observations were either based on human observers (unknown quality) or available only over a limited duration at limited locations, resulting in a severely statistics-limited set of coincidences with the CALIOP track.

{j_μ: Add a plot or table on layer geometry}

4 Results and data product availability

Geographic distributions of mean and median cloud base and thickness are shown in Figure 8 {j_μ: (which will be made from the CBASE data set when it's ready)}.

Comparison with 2B-GEOPROF-LIDAR cloud bases is shown in Figure 5. 2B-GEOPROF-LIDAR distinguishes between radar-only, lidar-only, and radar–lidar combined cloud bases; the latter category is rare for warm cloud and is not shown. For radar-only clouds, the mean error is large because the radar CBH predominantly clusters around the top of the ground clutter region with little dependence on the actual CBH. Lidar-only 2B-GEOPROF-LIDAR cloud base performs comparably to the CBASE cloud base on average; this is to be expected, as the underlying physical measurement is the same. Unlike 2B-GEOPROF-LIDAR, CBASE provides a validated uncertainty estimate, which allows an analysis to select only low-uncertainty cases or to statistically weight CBH according to uncertainty, as appropriate for the application.

Data {j_μ: for 2007 and 2008; do the other years later, perhaps with funding for the subadiabaticity study from somewhere} is available at DKRZ. {j_μ: Obtain DOI, put it here.}

5 Conclusions

We have presented the CBASE algorithm, which derives CBH from CALIOP lidar profiles. This algorithm produces CBH not only for thin clouds but also for clouds thick enough to attenuate the lidar (optical thickness $\tau \gtrsim 5$), based on the assumed homogeneity of cloud base height within an airmass. In addition to the CBH estimate, the CBASE algorithm supplies an expected uncertainty on the CBH. The CBASE data is available for the years 2007 and 2008 at {j_μ: insert DOI}.

CBASE CBH and its uncertainty have been evaluated using ground-based airport ceilometer data over the contiguous United States, using a data sample unbiased by the training of the algorithm. The evaluation showed that CBH and CBH uncertainty are unbiased at the better than 10% level: the bias on the CBH is 4%, and the bias on the uncertainty is 6%, both relative to the expected uncertainty.

The performance of CBASE CBH is similar to that of 2B-GEOPROF-LIDAR lidar-only CBH, which are based on the same underlying physical measurement. However, the validated CBH uncer-

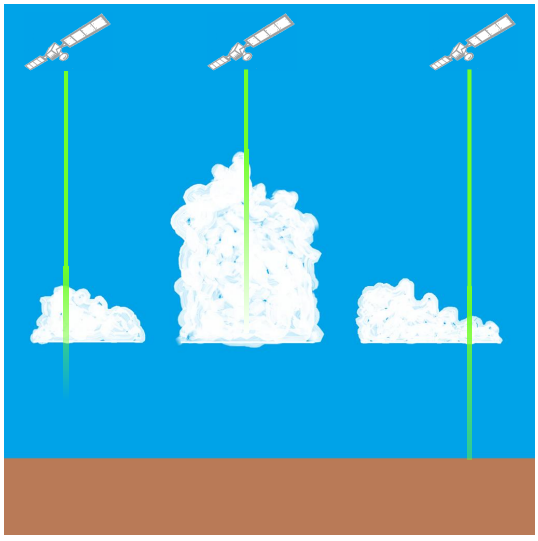

Figure 1. Schematic of CALIOP cloud base determination and evaluation strategy. In optically thick clouds, the lidar attenuates before reaching the cloud base, but the CBH of thin clouds can be used as a proxy for thick clouds in a cloud field with homogeneous CBH.

Figure 2. Scatter plots of CALIOP versus ceilometer local CBH faceted by the CALIOP VFM QA flag. Color indicates the number of CALIOP profiles within each bin of ceilometer and CALIOP CBH; black lines are contours of the empirical joint probability density; the red line is a linear least-squares fit, with 95% confidence interval shaded in light red; the blue line is a generalized additive model regression (Wood, 2004, 2011), with 95% confidence interval shaded in light blue; the dashed gray line is the one-to-one line. Statistics of the relationship between CALIOP and ceilometer base heights are provided in Table 1.

tainty provided by CBASE allows for selection of only accurate cloud base heights or for statistically weighting of CBH according to expected uncertainty. This, in turn, makes the CBASE CBH useful for pressing problems in climate research that require accurate knowledge of cloud geometry, such as cloud subadiabaticity, which will be presented in future work.

Acknowledgements. CALIOP VFM from ICARE. Computing (and data hosting?) at DKRZ. Funding.

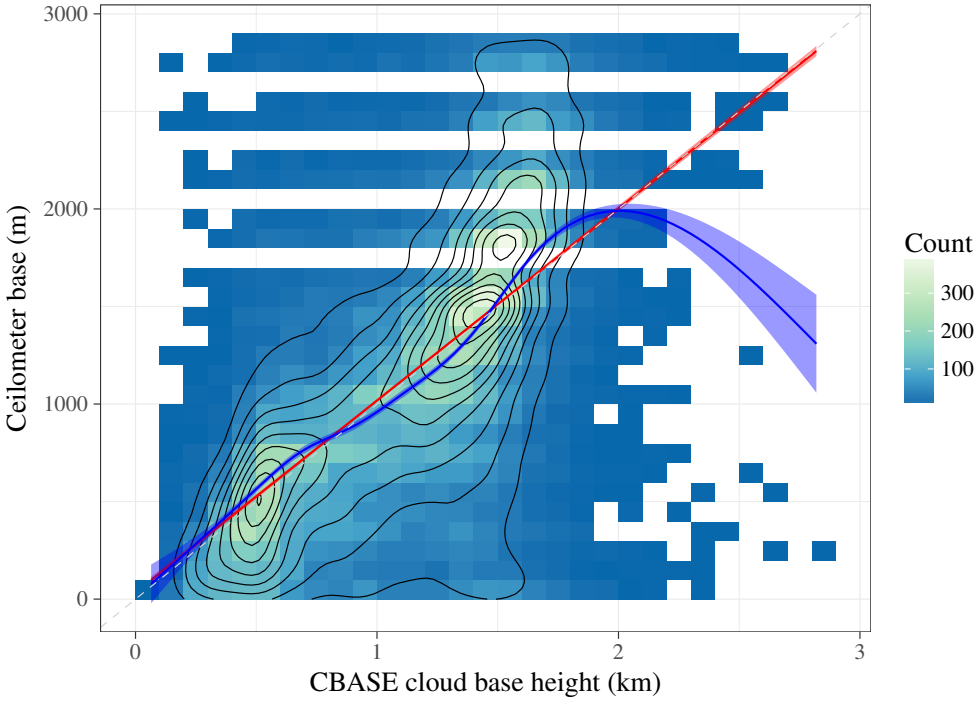

Figure 3. Scatter plot of CBASE versus ceilometer CBH; for description of the plot elements, see Figure 2. The linear fit has slope 0.98 and intercept 33.96 m.

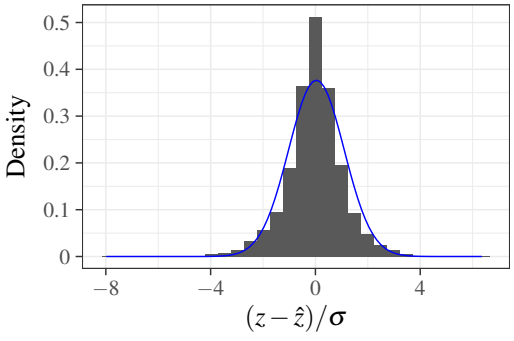

Figure 4. Distribution function of cloud base error divided by predicted uncertainty; for the ideal case of unbiased CBH and unbiased uncertainty, the distribution would be gaussian with zero mean and unit standard deviation. The superimposed least-squares gaussian fit (blue line) has mean 0.04 and standard deviation 1.06.

Table 1. Statistics of the relationship between ceilometer and CALIOP cloud base height faceted by CALIOP VFM QA flag. Shown are the number of CALIOP profiles n, the product-moment correlation coefficient r between CALIOP and ceilometer CBH, the RMSE, bias, and linear least-squares fit parameters.

```
## Error in select_impl(.data, vars): invalid column index : NA for
                    variable: 'group1' = 'group1'
```

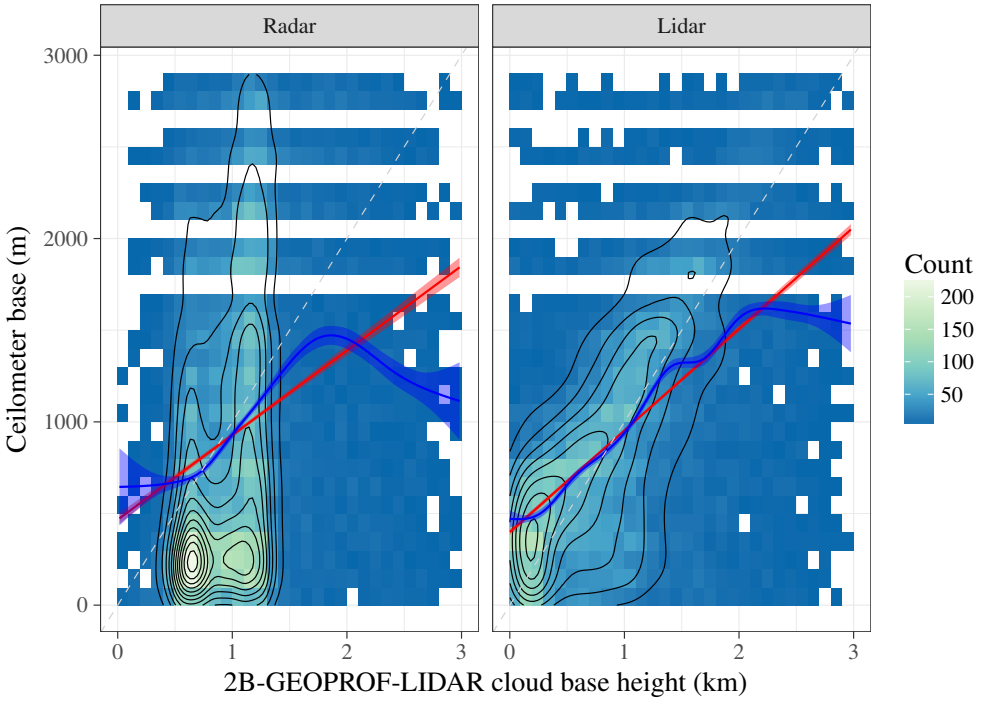

Figure 5. Scatter plot of 2B-GEOPROF-LIDAR versus ceilometer CBH faceted by the source of the cloud base (radar-only or lidar-only; due to their rare occurrence, combined radar–lidar base heights are not shown). For description of the plot elements, see Figure 2. Statistics of the relationship between 2B-GEOPROF-LIDAR and ceilometer base heights are provided in Table 3. {j_μ: I *think* this uses Claudia's algorithm (minimum cloud base within $D_{\max}$), but I have to check.}

Table 2. CBASE cloud base statistics by decile of predicted uncertainty; see Table 1 for a description of the statistics provided.

pred.rmse	n	r	RMSE (m)	bias (m)	fit
(167,427]	2624	0.741	404.	−46.9	$y = 1.03x + 28.0$ m
(427,453]	2624	0.719	429.	−28.4	$y = 1.06x - 32.0$ m
(453,469]	2624	0.703	461.	−18.8	$y = 1.09x - 87.7$ m
(469,484]	2624	0.685	463.	−17.8	$y = 1.03x - 18.3$ m
(484,497]	2624	0.628	506.	−6.06	$y = 0.976x + 33.4$ m
(497,508]	2624	0.574	547.	−8.73	$y = 0.986x + 25.5$ m
(508,522]	2624	0.596	547.	−14.1	$y = 1.01x + 5.37$ m
(522,541]	2624	0.572	562.	−9.26	$y = 0.967x + 49.6$ m
(541,573]	2624	0.502	639.	−22.7	$y = 0.939x + 96.8$ m
(573,748]	2624	0.447	720.	7.36	$y = 0.829x + 197.$ m

Table 3. Statistics of the relationship between ceilometer and 2B-GEOPROF-LIDAR CBH; see Table 1 for a description of the statistics provided.

flag.base	n	r	RMSE (m)	bias (m)	fit
Radar	15061	0.265	782.	98.1	$y = 0.461x + 466.$ m
Lidar	12813	0.564	594.	16.3	$y = 0.555x + 399.$ m

References

doi:10.1175/MWR-D-15-0242.1.

doi:10.1002/qj.828.

260 doi:10.1002/2013JD021374.

doi:10.1029/2007GL030347.

doi:10.1002/2013GL058970.

CALIPSO Science Team: CALIPSO/CALIOP Level 2, Vertical Feature Mask Data, version 4.10,
265 doi:10.5067/CALIOP/CALIPSO/LID_L2_VFM-Standard-V4-10, 2016.

National Oceanic and Atmospheric Administration, Department of Defense, Federal Aviation Administration, and United States Navy: Automated Surface Observing System User's Guide, http://www.nws.noaa.gov/asos/pdfs/aum-toc.pdf, 1998.

Wood, S. N.: Stable and efficient multiple smoothing parameter estimation for generalized additive models,
270 Journal of the American Statistical Association, 99, 673–686, 2004.

Wood, S. N.: Fast stable restricted maximum likelihood and marginal likelihood estimation of semiparametric generalized linear models, Journal of the Royal Statistical Society (B), 73, 3–36, 2011.

World Meteorological Organization: Techincal Regulations Volume II: Meteorological service for international air navigation, https://library.wmo.int/pmb_ged/wmo_49-v2_2013_en.pdf, 2013.

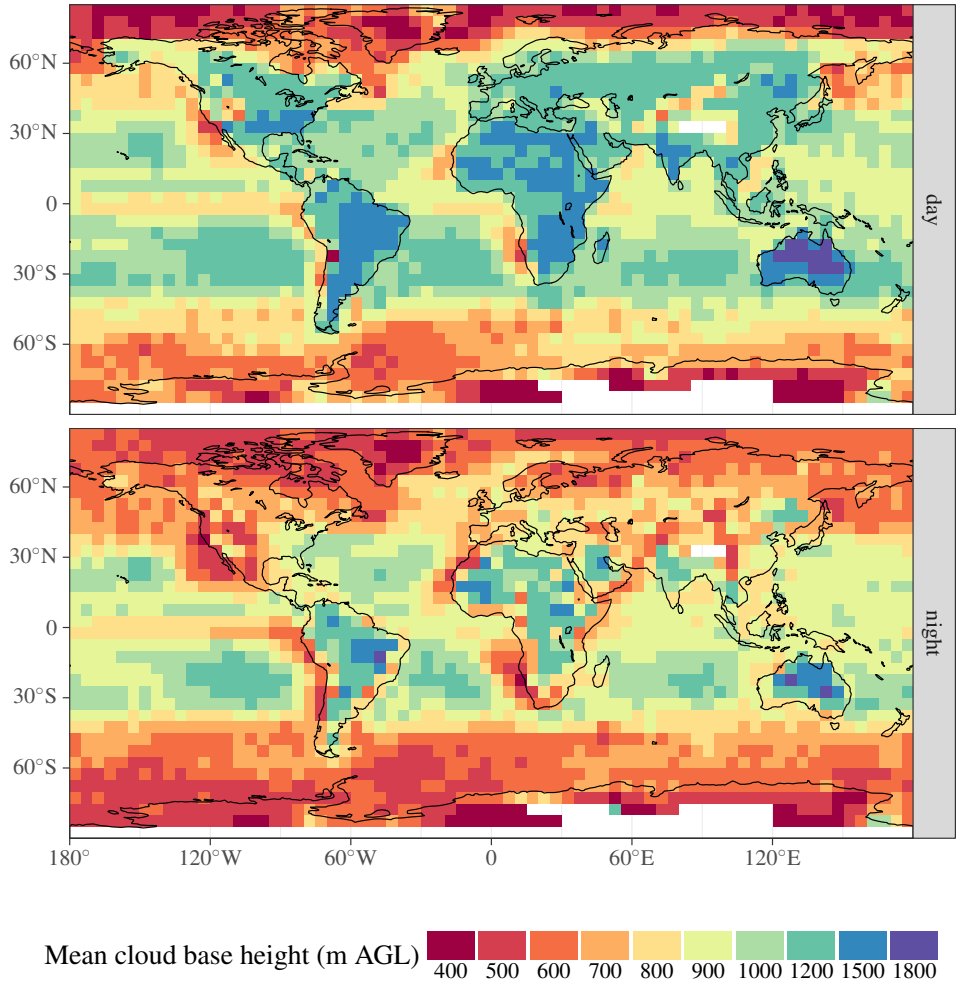

Figure 6. Geographic distribution of mean CBH above ground level. Statistics are calculated within each $5° \times 5°$ latitude–longitude box, and separately for CALIOP daytime and nighttime overpasses.

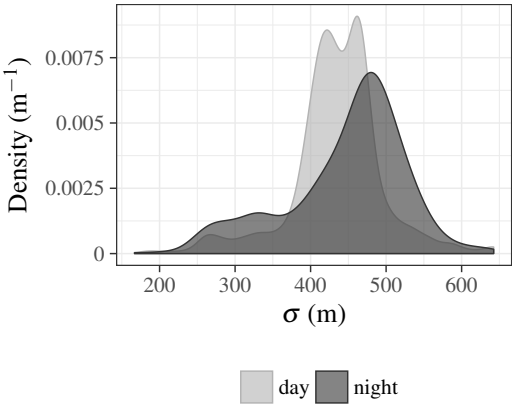

Figure 7. Distribution of predicted CBH uncertainty.

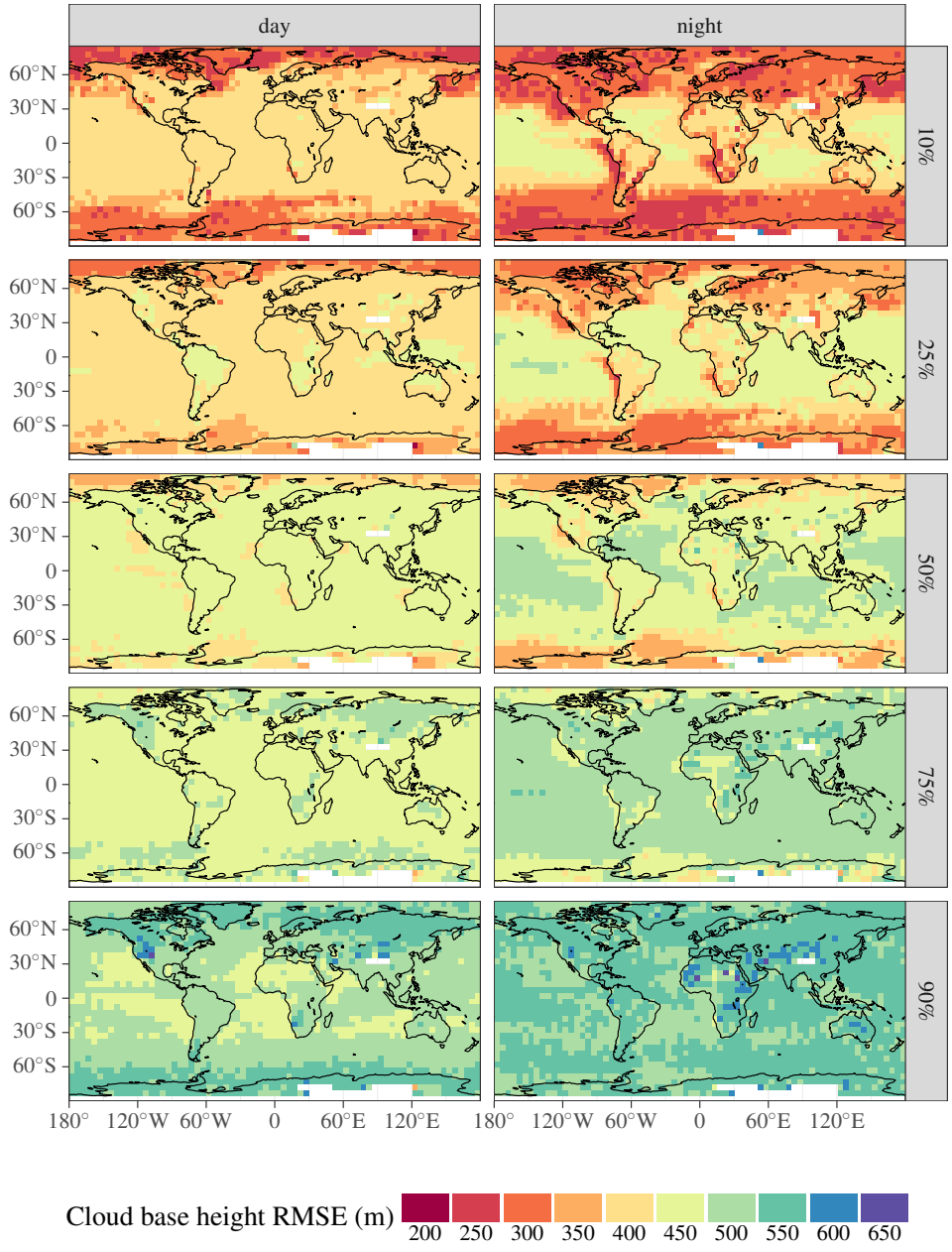

Figure 8. Cloud base uncertainty quantiles. Statistics are calculated within each 5° × 5° latitude–longitude box. The left (right) column shows statistics of daytime (nighttime) retrievals; daytime and nighttime are defined by the CALIOP VFM product.